INTERSPEECH 2023
20-24 August 2023, Dublin, Ireland

Low-complexity Broadband Beampattern Synthesis using Array Response Control

Jiayi Xu[1,2], *Jian Li*[1,2,*], *Weixin Meng*[1,2], *Xiaodong Li*[1,2], *Chengshi Zheng*[1,2]

[1]Key Laboratory of Noise and Vibration Research, Institute of Acoustics, Chinese Academy of Sciences, Beijing, China
[2]University of Chinese Academy of Sciences, Beijing, China
{xujiayi, lijian, mengweixin, lxd, cszheng}@mail.ioa.ac.cn

Abstract

Beampattern synthesis plays a critical role in fixed beamforming. A fast beampattern synthesis method is highly desired, especially for broadband beamformers requiring a large number of weight parameters for better performance. This paper proposes a low-complexity broadband beampattern synthesis method for time-domain beamformers. Introducing the null-forming scheme of adaptive beamformers, a virtual interference-plus-noise matrix is iteratively constructed to control the sidelobe pattern accurately. The proposed method reduces the computational complexity when compared with the existing algorithms based on the interior-point method (IPM), especially for large-scale microphone arrays. Simulation results demonstrate that the proposed method obtains equivalent beampatterns with much higher efficiency than the IPM-based method. In speech extraction experiments, the designed beamformers exhibit better suppression performance than the conventional fixed beamformer.

Index Terms: beampattern synthesis, microphone array, sidelobe control

1. Introduction

Microphone array beamforming techniques generally aim to form a strong beam toward the direction of interest while suppressing interference and environmental noise, which have been utilized in various audio applications such as speech communication, machine-human interaction, and sound field analysis [1, 2]. In broadband applications, beamformers are performed in either the frequency domain or time domain [3–5]. Compared with frequency-domain beamformers which require narrowband decomposition and block processing, time-domain beamformers that adopt a filter-and-sum structure are sometimes preferred for lower processing delay. Beamformers can be roughly divided into adaptive and fixed beamformers according to whether the weight vector depends on the received signals. Generally, a fixed beamformer cannot automatically adapt the weight vector when the interference and noise spatial characteristics change. However, it is still worth studying because of its much higher robustness and lower computational complexity than an adaptive beamformer in most cases [6, 7]. For fixed beamformers, designing beampattern under specific requirements is a basic problem. This paper focuses on broadband beampattern synthesis for time-domain beamformers.

In the past decades, extensive research has been devoted to broadband beampattern synthesis, such as differential beamforming [8–10], modal beamforming [11, 12] and optimization techniques [13–18]. Among those methods, optimization techniques exhibit superiority in obtaining optimal weight vectors. Yan *et al.* formulated the beampattern synthesis problem into a second-order cone programming (SOCP) problem [14, 15], which can be solved by the well-established interior-point method (IPM) [13] using some toolboxes such as SEDUMI [19] and CVX [20]. Chen [16] proposed a SOCP-based near-field broadband beampattern synthesis method, which is robust against errors of microphone array characteristics. In more recent years, the alternating direction method of multipliers has been introduced for lower computational complexity and better convergence [17, 18]. Nevertheless, even a slight change in the constraints requires a redesign of the beamformer for the above methods based on optimization algorithms, leading to a high computational load.

Besides the optimization techniques, the null-forming scheme of adaptive beamformers has also shown impressive performance in narrowband beampattern synthesis [21–25]. Olen and Compton proposed adjusting the sidelobe pattern by adding virtual interferences, while the iteration of the interference power is computationally inefficient [21]. Zhang *et al.* proposed an optimal and precise array response control (OPARC) method by constructing a virtual interference-plus-noise covariance matrix (VINCM) [24]. However, the above techniques focus on narrowband applications, null-forming based broadband pattern synthesis methods for time-domain beamformers have yet to be developed.

To achieve fast and accurate beampattern synthesis for time-domain beamformers, this paper proposes precise broadband array response control (PBARC). By adding virtual interference and choosing the appropriate interference power, the array response is accurately controlled using the adaptive null-forming scheme. Accordingly, the VINCM is iteratively constructed, and the update form of the weight vector is derived. The update of the VINCM is additionally simplified by introducing the matrix inversion lemma, leading to much less complexity in each iteration than that of the IPM-based method. Simulation examples illustrate the effectiveness of the PBARC method, the average runtime compared with the IPM-based method further demonstrates its efficiency. In speech extraction experiments, the beamformers designed using PBARC obtain higher perceptual evaluation scores than the conventional fixed beamformers, exhibiting better performance in suppressing the interference and extracting the desired speech signal.

2. Broadband signal model and problem formulation

Consider a time-domain beamformer with M sensors, each element is followed by a finite impulse response (FIR) filter with L real-valued tap weights, and the outputs of each FIR filter

*Jian Li is the corresponding author.

10.21437/Interspeech.2023-634

are summed up for the beamformer output. Denote the lth tap weight of the mth filter as $h_{m,l}$, the real-valued weight vector of time-domain beamformers is arranged as

$$\mathbf{h} = [h_{1,1}, h_{2,1}, \ldots, h_{M,1}, \ldots, h_{1,L}, h_{2,L}, \ldots, h_{M,L}]^{\mathrm{T}} \quad (1)$$

where $[\cdot]^{\mathrm{T}}$ denotes the transpose operation. The steering vector of time-domain beamformers is given by $\mathbf{u}(f,\Omega) = \mathbf{e}(f) \otimes \mathbf{a}(f,\Omega)$, where f is the frequency, $\Omega = (\theta,\phi)$ consists of the azimuth angle θ and elevation angle ϕ, $\otimes$ denotes the Kronecker product. $\mathbf{e}(f)=[1, e^{-j2\pi f/f_s}, \ldots, e^{-j2\pi(L-1)f/f_s}]^{\mathrm{T}} \in \mathbb{C}^L$ is the Fourier transform operator, f_s is the sampling frequency. The frequency-domain steering vector $\mathbf{a}(f,\Omega) \in \mathbb{C}^M$ is $\mathbf{a}(f,\Omega) = [e^{-j2\pi f\tau_1(\Omega)}, \ldots, e^{-j2\pi f\tau_M(\Omega)}]^{\mathrm{T}}$, $\tau_m(\Omega)$ is the time-delay between the mth element and the reference location. The normalized power response is given by

$$P(f,\Omega) = |\mathbf{h}^{\mathrm{T}}\mathbf{u}(f,\Omega)|^2 \Big/ |\mathbf{h}^{\mathrm{T}}\mathbf{u}(f_0,\Omega_0)|^2 \quad (2)$$

Ω_0 is the look direction, f_0 is chosen in the passband.

In the presence of directional interference and white noise, the interference-plus-noise covariance matrix of broadband signals is given by

$$\begin{aligned}\mathbf{R}_{\mathrm{i+n}} = & \int\limits_{\Omega\in\Theta_i} \Big[\int_{f_l}^{f_u} \tfrac{S(f,\Omega)}{2}\mathbf{u}(f,\Omega)\mathbf{u}^{\mathrm{H}}(f,\Omega)\mathrm{d}f + \\ & \int_{-f_u}^{-f_l} \tfrac{S(f,\Omega)}{2}\mathbf{u}(f,\Omega)\mathbf{u}^{\mathrm{H}}(f,\Omega)\mathrm{d}f\Big]\mathrm{d}\Omega + \sigma_{\mathrm{n}}^2\mathbf{I}_{ML} \\ = & \int\limits_{\Omega\in\Theta_{\mathrm{i}}} \int_{f_{\mathrm{l}}}^{f_{\mathrm{u}}} S(f,\Omega)\left[\Re\{\mathbf{u}(f,\Omega)\}\Re\{\mathbf{u}^{\mathrm{T}}(f,\Omega)\}+\right. \\ & \left.\Im\{\mathbf{u}(f,\Omega)\}\Im\{\mathbf{u}^{\mathrm{T}}(f,\Omega)\}\right]\mathrm{d}f\mathrm{d}\Omega + \sigma_{\mathrm{n}}^2\mathbf{I}_{ML}\end{aligned} \quad (3)$$

where σ_{n}^2 is the noise power and $\mathbf{I}_{ML} \in \mathbb{R}^{ML\times ML}$ is an identity matrix. The interference power $S(f,\Omega)$ is symmetrical according to the Fourier transform property, Θ_i is the angle range of interference, f_l and f_u are respectively the lower and upper bounds of the frequency band. $\Re\{\cdot\}$ and $\Im\{\cdot\}$ respectively extract the real and imaginary parts, $(\cdot)^{\mathrm{H}}$ denotes the conjugate transpose operation.

For a beamformer aimed to minimize the output interference and noise power with distortionless response at Ω_0, the optimization problem is formulated as

$$\begin{aligned}&\min_{\mathbf{h}} \mathbf{h}^{\mathrm{T}}\mathbf{R}_{\mathrm{i+n}}\mathbf{h} \\ &\text{s.t. } \mathbf{C}^{\mathrm{T}}(\Omega_0)\,\mathbf{h}=\mathbf{g}\end{aligned} \quad (4)$$

The constraint $\mathbf{C}^{\mathrm{T}}(\Omega_0)\mathbf{h}=\mathbf{g}$ restrains the look-direction response $P(f_k,\Omega_0)(1 \le k \le K)$ to be unitary, K is the number of controlled frequencies. The matrix $\mathbf{C}(\Omega_0) = [\Re\{\mathbf{u}(f_1,\Omega_0),\ldots,\mathbf{u}(f_K,\Omega_0)\}, \Im\{\mathbf{u}(f_1,\Omega_0),\ldots,\mathbf{u}(f_K,\Omega_0)\}]$ is an $ML \times 2K$ real-valued matrix, $\mathbf{g} = [1,\ldots,1,0,\ldots,0]^{\mathrm{T}}$ consists of K ones and K zeros. Consequently, the look-direction response $|\mathbf{h}^{\mathrm{T}}\mathbf{u}(f_k,\Omega_0)|^2 = |\mathbf{h}^{\mathrm{T}}[\Re(\mathbf{u}(f_k,\Omega_0)) + \Im(\mathbf{u}(f_k,\Omega_0))]|^2 = 1 (1 \le k \le K)$.

Solved by the Lagrange multiplier method, the closed-form solution of (4) is given by

$$\mathbf{h} = \mathbf{R}_{\mathrm{i+n}}^{-1}\mathbf{C}(\Omega_0)\left[\mathbf{C}^{\mathrm{T}}(\Omega_0)\mathbf{R}_{\mathrm{i+n}}^{-1}\mathbf{C}(\Omega_0)\right]^{-1}\mathbf{g} \quad (5)$$

where $(\cdot)^{-1}$ denotes matrix inverse operation.

3. Precise broadband array response control

Although the existing methods based on optimization techniques obtain optimal weight vectors, the computational burden limits their wide applications. Especially for large-scale arrays utilized in outdoor long-distance speech extraction and other complicated environments, the computational costs grow significantly with the increase in the number of microphones. This motivates us to propose a low-complexity beampattern synthesis method by introducing the null-forming scheme of adaptive beamformers and updating the weight vector iteratively.

The PBARC algorithm consists of the initialization and iteration stages. In the initialization stage, the VINCM is set as $\mathbf{R}_{v,0} = \mathbf{I}_{ML}$ to avoid the difficulties of inverting a singular matrix. In the iteration stage, each update includes two steps: 1) select the controlling location in the sidelobe region, and compute the update form of $\mathbf{h}$ using the matrix inversion lemma to reduce the computational complexity; 2) calculate the virtual interference power to control the response precisely. The two steps are described in detail in the following two parts.

3.1. Calculation of the update form for the weight vector

Because it is well-known that adaptive beamformers automatically form a null to suppress a directional interference, the proposed method searches the maximum peak in the sidelobe region and controls the response by adding a virtual interference. After the $(i-1)$th iteration, $\mathbf{R}_{v,i-1}$ denotes the current VINCM. In the ith iteration, if (f_i,Ω_i) is selected as the controlling location, $\mathbf{R}_{v,i}$ is updated according to (3) by

$$\begin{aligned}\mathbf{R}_{v,i} = & \mathbf{R}_{v,i-1} + S_i\left[\Re\{\mathbf{u}(f_i,\Omega_i)\}, \Im\{\mathbf{u}(f_i,\Omega_i)\}\right]\cdot \\ & \left[\Re\{\mathbf{u}(f_i,\Omega_i)\}, \Im\{\mathbf{u}(f_i,\Omega_i)\}\right]^{\mathrm{T}}\end{aligned} \quad (6)$$

where $\mathbf{u}(f_i,\Omega_i)$ is the steering vector of the newly-added virtual interference, S_i is the interference power. However, inverting $\mathbf{R}_{v,i}$ in (5) requires complexity of $\mathrm{O}(M^3L^3)$, which costs high complexity especially for large-scale microphone arrays. To reduce the complexity, we introduce the matrix inversion lemma to transform the matrix inverse operation into a series of low-complexity arithmetic, including second-order eigenvalue decomposition, multiplications, and summations. Therefore, $\mathbf{R}_{v,i}^{-1}$ is updated by

$$\mathbf{R}_{v,i}^{-1} = \mathbf{R}_{v,i-1}^{-1} - \frac{S_i\mathbf{p}_{1,i}\mathbf{p}_{1,i}^{\mathrm{T}}}{\lambda_{1,i}S_i+1} - \frac{S_i\mathbf{p}_{2,i}\mathbf{p}_{2,i}^{\mathrm{T}}}{\lambda_{2,i}S_i+1} \quad (7)$$

where

$$[\mathbf{p}_{1,i},\mathbf{p}_{2,i}] = \mathbf{R}_{v,i-1}^{-1}\left[\Re\{\mathbf{u}(f_i,\Omega_i)\}, \Im\{\mathbf{u}(f_i,\Omega_i)\}\right]\mathbf{E}_i \quad (8a)$$

$$\begin{aligned}\mathbf{E}_i\begin{bmatrix}\lambda_{1,i} & 0\\ 0 & \lambda_{2,i}\end{bmatrix}\mathbf{E}_i^{\mathrm{T}} = & \left[\Re\{\mathbf{u}(f_i,\Omega_i)\}, \Im\{\mathbf{u}(f_i,\Omega_i)\}\right]^{\mathrm{T}}\cdot \\ & \mathbf{R}_{v,i-1}^{-1}\left[\Re\{\mathbf{u}(f_i,\Omega_i)\}, \Im\{\mathbf{u}(f_i,\Omega_i)\}\right]\end{aligned} \quad (8b)$$

Equation (8b) is the eigenvalue decomposition of the 2×2 matrix on the right-hand side, $\mathbf{E}_i$ consists of the eigenvectors, $\lambda_{1,i}$ and $\lambda_{2,i}$ are the two eigenvalues. Using (7), the matrix inverse operation is avoided, the computational complexity of updating $\mathbf{R}_{v,i-1}^{-1}$ reduces from $\mathrm{O}(M^3L^3)$ to $\mathrm{O}\left(M^2L^2\right)$.

Similarly, $\left[\mathbf{C}^{\mathrm{T}}(\Omega_0)\mathbf{R}_{v,i}^{-1}\mathbf{C}(\Omega_0)\right]^{-1} \in \mathbb{R}^{2K\times 2K}$ is updated using the matrix inversion lemma as

$$\begin{aligned}\left[\mathbf{C}^{\mathrm{T}}(\Omega_0)\mathbf{R}_{v,i}^{-1}\mathbf{C}(\Omega_0)\right]^{-1} = & \left[\mathbf{C}^{\mathrm{T}}(\Omega_0)\mathbf{R}_{v,i-1}^{-1}\mathbf{C}(\Omega_0)\right]^{-1} + \\ & \frac{S_i\mathbf{q}_{1,i}\mathbf{q}_{1,i}^{\mathrm{T}}}{(\lambda_{1,i}-\gamma_{1,i})S_i+1} + \frac{S_i\mathbf{q}_{2,i}\mathbf{q}_{2,i}^{\mathrm{T}}}{(\lambda_{2,i}-\gamma_{2,i})S_i+1}\end{aligned} \quad (9)$$

where

$$\begin{aligned}[\mathbf{q}_{1,i},\mathbf{q}_{2,i}] = & \left[\mathbf{C}^{\mathrm{T}}(\Omega_0)\mathbf{R}_{v,i-1}^{-1}\mathbf{C}(\Omega_0)\right]^{-1}\cdot \\ & \mathbf{C}^{\mathrm{T}}(\Omega_0)[\mathbf{p}_{1,i},\mathbf{p}_{2,i}]\,\mathbf{F}_i\end{aligned} \quad (10a)$$

$$\begin{aligned}\mathbf{F}_i\begin{bmatrix}\gamma_{1,i} & 0\\ 0 & \gamma_{2,i}\end{bmatrix}\mathbf{F}_i^{\mathrm{T}} = & [\mathbf{p}_{1,i},\mathbf{p}_{2,i}]^{\mathrm{T}}\mathbf{C}(\Omega_0)\cdot \\ & \left[\mathbf{C}^{\mathrm{T}}(\Omega_0)\mathbf{R}_{v,i-1}^{-1}\mathbf{C}(\Omega_0)\right]^{-1}\mathbf{C}^{\mathrm{T}}(\Omega_0)\cdot[\mathbf{p}_{1,i},\mathbf{p}_{2,i}]\end{aligned} \quad (10b)$$

Equation (10b) is the eigenvalue decomposition of the 2×2 matrix on the right-hand side, where $\mathbf{F}_i$ consists of the eigenvectors, $\gamma_{1,i}$ and $\gamma_{2,i}$ are the two eigenvalues.

Substituting (7) and (9) into (5), $\mathbf{h}_i$ is updated as

$$\mathbf{h}_i = \left[\mathbf{R}_{v,i-1}^{-1} - \frac{S_i \mathbf{p}_{1,i}\mathbf{p}_{1,i}^{\mathrm{T}}}{\lambda_{1,i}S_i+1} - \frac{S_i \mathbf{p}_{2,i}\mathbf{p}_{2,i}^{\mathrm{T}}}{\lambda_{2,i}S_i+1}\right] \cdot \mathbf{C}(\Omega_0)\left\{\left[\mathbf{C}^{\mathrm{T}}(\Omega_0)\mathbf{R}_{v,i-1}^{-1}\mathbf{C}(\Omega_0)\right]^{-1} + \frac{S_i \mathbf{q}_{1,i}\mathbf{q}_{1,i}^{\mathrm{T}}}{(\lambda_{1,i}-\gamma_{1,i})S_i+1} + \frac{S_i \mathbf{q}_{2,i}\mathbf{q}_{2,i}^{\mathrm{T}}}{(\lambda_{2,i}-\gamma_{2,i})S_i+1}\right\}\mathbf{g} \quad (11)$$

In (11), S_i is the only unknown factor, which can be extracted for a more concise expression. Thus, the update of $\mathbf{h}_i$ (11) is formulate as a quartic equation of S_i

$$\mathbf{h}_i = z_i \mathbf{J}_i \left[(S_i)^4, (S_i)^3, (S_i)^2, S_i, 1\right]^{\mathrm{T}} \quad (12)$$

where $z_i = 1/\{(\lambda_{1,i}S_i+1)(\lambda_{2,i}S_i+1)[(\lambda_{1,i}-\gamma_{1,i})S_i+1][(\lambda_{2,i}-\gamma_{2,i})S_i+1]\}$ is the product of the denominators, $\mathbf{J}_i \in \mathbb{R}^{ML\times 5}$ is a determined matrix calculated by directly extracting S_i and z_i in (11), which is not presented in this paper due to its complicated expression and the limited pages. S_i is determined in the following part to control the array response accurately.

3.2. Determination of the interference power

For adaptive beamformers, the null depth grows with the increase of the interference power, thus selecting an appropriate S_i achieves accurate response control. Substitute (12) into (2) and set the desired response as ρ_i, the equation is then formulated as

$$\mathbf{h}_i^{\mathrm{T}}\mathbf{u}(f_i,\Omega_i)\mathbf{u}^{\mathrm{H}}(f_i,\Omega_i)\mathbf{h}_i - \rho_i \mathbf{h}_i^{\mathrm{T}}\mathbf{u}(f_0,\Omega_0)\mathbf{u}^{\mathrm{H}}(f_0,\Omega_0)\mathbf{h}_i = 0 \quad (13)$$

Equation (13) can be further simplified as

$$\left[(S_i)^4, (S_i)^3, (S_i)^2, S_i, 1\right]\mathbf{G}_i\left[(S_i)^4, (S_i)^3, (S_i)^2, S_i, 1\right]^{\mathrm{T}} = 0 \quad (14)$$

where the nonzero factor z_i is omitted, $\mathbf{G}_i \in \mathbb{C}^{5\times 5}$ is given by

$$\mathbf{G}_i = \mathbf{J}_i^{\mathrm{T}}\left[\mathbf{u}(f_i,\Omega_i)\mathbf{u}^{\mathrm{H}}(f_i,\Omega_i) - \rho_i \mathbf{u}(f_0,\Omega_0)\mathbf{u}^{\mathrm{H}}(f_0,\Omega_0)\right]\mathbf{J}_i \quad (15)$$

Since $\mathbf{u}(f_i,\Omega_i)\mathbf{u}^{\mathrm{H}}(f_i,\Omega_i) - \rho_i \mathbf{u}(f_0,\Omega_0)\mathbf{u}^{\mathrm{H}}(f_0,\Omega_0)$ ranks no more than 2, $\mathbf{G}_i$ accordingly ranks no more than 2. Using the eigenvalue decomposition $\mathbf{G}_i = \mathbf{W}_i\mathbf{\Sigma}_i\mathbf{W}_i^{\mathrm{H}}$, $\mathbf{G}_i = \mathbf{W}_{i,1}\mathbf{\Sigma}_i(1,1)\mathbf{W}_{i,1}^{\mathrm{T}} + \mathbf{W}_{i,2}\mathbf{\Sigma}_i(2,2)\mathbf{W}_{i,2}^{\mathrm{T}}$, where $\mathbf{W}_{i,n}(n = 1,2)$ represents the nth eigenvector of $\mathbf{W}_i$. Equation (14) can be simplified as

$$\begin{aligned}&[(S_i)^4, (S_i)^3, (S_i)^2, S_i, 1]\mathbf{W}_{i,1}\mathbf{\Sigma}_i(1,1)\mathbf{W}_{i,1}^{\mathrm{T}}\cdot\\ &[(S_i)^4, (S_i)^3, (S_i)^2, S_i, 1]^{\mathrm{T}} + [(S_i)^4, (S_i)^3, (S_i)^2, S_i, 1]\cdot\\ &\mathbf{W}_{i,2}\mathbf{\Sigma}_i(2,2)\mathbf{W}_{i,2}^{\mathrm{T}}[(S_i)^4, (S_i)^3, (S_i)^2, S_i, 1]^{\mathrm{T}} = 0\end{aligned} \quad (16)$$

which can be simplified into two quartic equations as

$$\left[(S_i)^4, (S_i)^3, (S_i)^2, S_i, 1\right] \cdot \left(\sqrt{\mathbf{\Sigma}_i(1,1)}\mathbf{W}_{i,1} - \sqrt{-\mathbf{\Sigma}_i(2,2)}\mathbf{W}_{i,2}\right) = 0 \quad (17a)$$

$$\left[(S_i)^4, (S_i)^3, (S_i)^2, S_i, 1\right] \cdot \left(\sqrt{\mathbf{\Sigma}_i(1,1)}\mathbf{W}_{i,1} + \sqrt{-\mathbf{\Sigma}_i(2,2)}\mathbf{W}_{i,2}\right) = 0 \quad (17b)$$

In (17), each quartic equation obtains four closed-form solutions. Because the array response decreases monotonously with the increase of S_i, there is only one feasible solution for the real-valued factor S_i. Consequently, only the real-valued solution is reserved among the eight solutions of (17). The proposed method is summarized in Table 1.

Table 1: *Summary of the proposed PBARC method*

Input	Calculate the initial $\mathbf{h}_i(i=0)$ using (5), where $\mathbf{R}_{v,0} = \mathbf{I}_{ML}$.
1:	**for** i=1,2,..., **do**
2:	Calculate the beampattern of $\mathbf{h}_{i-1}$ using (2), select the maximum peak in the sidelobe region as the next controlling location;
3:	Calculate $\mathbf{G}_i$ using (15), solve (17) for S_i;
4:	Update $\mathbf{h}_i$ using (12);
5:	Update $\mathbf{R}_{v,i}^{-1}$ and $\left[\mathbf{C}^{\mathrm{T}}(\Omega_0)\mathbf{R}_{v,i}^{-1}\mathbf{C}(\Omega_0)\right]^{-1}$ using (7) and (9);
6:	**end for**
Output	The weight vector $\mathbf{h}_i$.

3.3. Computational complexity analysis

The computational complexity of the proposed method and the IPM-based method is described by the number of floating-point operations [26]. The initialization and each iteration are respectively evaluated. In the initialization, both methods calculate the steering vectors, and the PBARC algorithm requires to compute $\mathbf{h}_0$ which needs comparatively smaller complexity. The computational complexity comparison results are presented in Table 2, where N_Ω is the number of grids in the sidelobe region. For each iteration, the computational complexity of the PBARC method is much smaller than that of the IPM-based method. Besides the complexity of each iteration, the number of iterations also plays an essential role in the total runtime. To evaluate the overall complexity, the average runtime of the two methods is compared in the next section.

Table 2: *The computational complexity*

Method	IPM-based	PBARC
Initialization	$\mathrm{O}(N_\Omega KML)$	$\mathrm{O}(N_\Omega KML)$
Each iteration	$\mathrm{O}(N_\Omega KM^2L^2)$	$\mathrm{O}(N_\Omega KML) + \mathrm{O}\left(M^2L^2\right)$

4. Simulation

4.1. Beampattern synthesis

In this section, beampattern synthesis simulations for linear and rectangular arrays under different design requirements are provided to illustrate the effectiveness of the PBARC algorithm.

First, consider a 12-element array with 30-tap FIR filters, the inter-element spacing is 2.8 cm. The elevation angle is fixed as $\phi = 0^\circ$, the azimuth angle range $\theta \in [-90^\circ, 90^\circ]$ is discretized with an interval of 2°, the frequency band $f \in [2000, 7500]$ Hz is discretized with an interval of 250 Hz. The look direction $\theta_0 = 0^\circ$, the desired pattern is set as the uniform sidelobe with a sidelobe level (SLL) of -30 dB. Beampatterns of the initial beamformer and beamformers of the 20th, 50th, and 100th iterations are presented in Figure 1, where the sidelobe pattern gradually converges to the desired SLL with the increasing number of the iteration.

The PBARC method additionally achieves null-forming beampattern synthesis. A -20 dB uniform sidelobe pattern with a null at -60° is desired, the depth is -40 dB and the width is 4°. The beampatterns of the IPM-based and PBARC methods are compared in Figure 2. The desired beampattern of the IPM-based method is chosen as the obtained pattern of PBARC to guarantee the similarity of the designed beampatterns. Both the IPM-based method and PBARC method design beampatterns that meet the requirements, achieving effective beampattern synthesis performance.

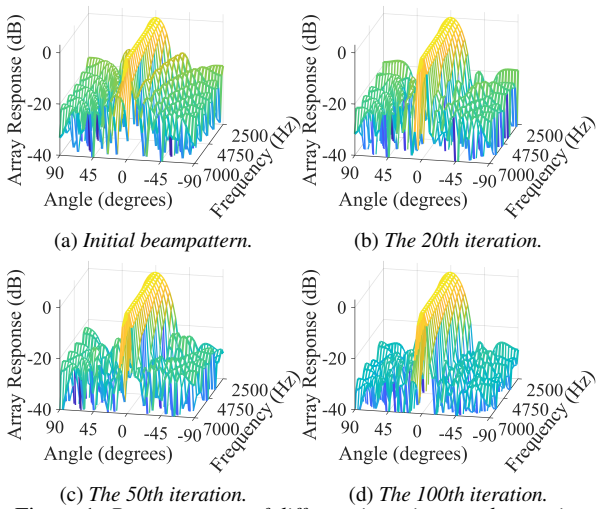

(a) *Initial beampattern.* (b) *The 20th iteration.*

(c) *The 50th iteration.* (d) *The 100th iteration.*

Figure 1: *Beampatterns of different iteration numbers using the PBARC method.*

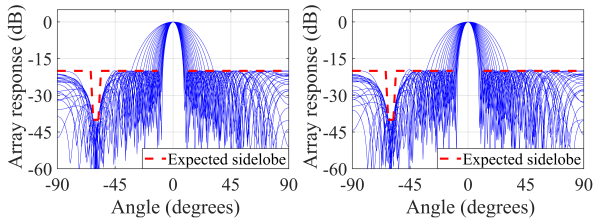

(a) *The IPM-based method.* (b) *The PBARC method.*

Figure 2: *Null-forming for the linear array using different methods.*

Second, beampattern synthesis for a rectangular array is evaluated. Consider an array with 12×6 elements, the spacing of the 12-element and 6-element sides are respectively 2.8 cm and 5 cm, each FIR filter consists of 30 taps. The elevation angle range $\phi \in [0°, 90°]$ and the azimuth angle range $\theta \in [-90°, 90°]$ are both discretized with an interval of $5°$, the frequency band $f \in [1000, 3500]$ Hz is discretized with an interval of 250 Hz. The look direction $\phi_0 = 0°$, the SLL is set as -15 dB, a -25 dB null is desired in $(\theta, \phi) = (0°, 50°)$. The designed beampatterns in 1500 Hz and 2500 Hz are shown in Figure 3, which validates the effectiveness of PBARC in beampattern synthesis for two-dimensional arrays.

Third, the average runtime of the IPM-based and PBARC methods under different design requirements are compared. Computations are performed on a computer with an Intel Core i5 processor of speed 2.5 GHz and 16 GB RAM, each result is obtained by averaging the results of 20 Monte-Carlo experiments. In the design of -30 dB uniform sidelobe pattern (Figure 1) and null-forming (Figure 2) for the linear array, the IPM-based method respectively requires 19.08 s and 19.22 s, while the PBARC method requires 4.74 s and 3.06 s. As for the null-forming (Figure 3) of the rectangular array, the IPM-based and PBARC methods need 2300.75 s and 33.46 s, respectively. As the PBARC method achieves similar designs to the IPM-based method, it requires much less runtime. Especially for arrays with a large number of microphones, the PBARC method increases the efficiency more significantly.

4.2. Evaluation in speech extraction

In this part, the designed beamformers of the 72-element rectangular arrays are evaluated by speech extraction tasks, together

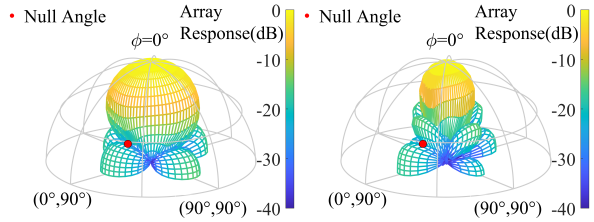

(a) *1500 Hz.* (b) *2500 Hz.*

Figure 3: *Null-forming for the rectangular array using the PBARC method.*

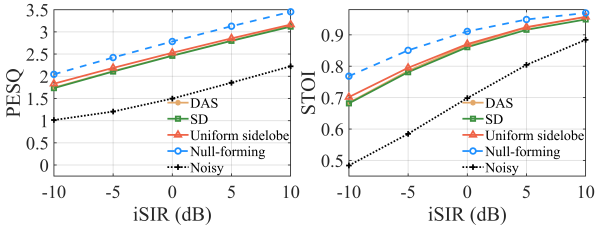

(a) *PESQ.* (b) *STOI.*

Figure 4: *The simulation results.*

with the delay-and-sum (DAS) beamformer and superdirective (SD) beamformer for comparison. The SLL in [1200,3500] Hz is designed as -20 dB for the uniform sidelobe beamformer, an SLL of -15 dB in [1000,3500] Hz and a null of -20 dB in [500,3500] Hz are desired for the null-forming beamformer.

Set the reverberation time as $T_{60} = 130$ ms, the room impulse response is generated with the well-known image method [27]. The room size is 6 m $\times$ 7 m $\times$ 3 m, both the target and interference are 2 m away from the microphone array and at the same height as the array. Each simulation experiment includes one target and one interference selected from $\Theta_n = \{\pm 50°, \pm 60°, \pm 70°, \pm 80°, \pm 90°\}$, the look direction is $0°$. The target signals are selected from the TIMIT dataset [28] of 15 men and 15 women, the interference is the white noise signal chosen from the NOISEX-92 dataset [29]. The microphone self-noise is white additive Gaussian noise with a signal-to-noise ratio (SNR) of 30 dB.

The perceptual evaluation of speech quality (PESQ) [30] and short-time objective intelligibility (STOI) [31] are utilized to evaluate speech quality. The average results of 30 subjects and 12 interference directions in Θ_n are shown in Figure 4. Among the four beamformers, the beamformer with null-forming shows the best performance in different input signal-to-interference ratios (iSIR), demonstrating its effectiveness in interference suppression.

5. Conclusions

This paper introduces the null-forming scheme of adaptive beamformers into broadband beampattern synthesis and achieves precise array response control. Several design examples are provided to illustrate the effectiveness and efficiency of the proposed method, the performance in speech extraction is also evaluated by simulation experiments. In the near future, we will introduce the PBARC method into frequency-invariant beampattern synthesis and evaluate its practical performance by actual experiments using a microphone array.

6. Acknowledgements

This work was supported by the National Natural Science Foundation of China under Grant No.62001467.

7. References

[1] J. Benesty, J. Chen, and Y. Huang, *Microphone Array Signal Processing*. Berlin, Germany: Springer-Verlag, 2008.

[2] H. Sun, S. Yan, and U. P. Svensson, "Optimal higher order ambisonics encoding with predefined constraints," *IEEE Trans. Audio, Speech, Lang. Process.*, vol. 20, no. 3, pp. 742–754, Mar. 2012.

[3] W. Liu and S. Weiss, *Wideband Beamforming: Concepts and Techniques*. Chichester, U.K.: Wiley, 2010.

[4] O. L. Frost, "An algorithm for linearly constrained adaptive array processing," *Proceedings of the IEEE*, vol. 60, no. 8, pp. 926–935, Aug. 1972.

[5] S. Yan, C. Hou, X. Ma, and Y. Ma, "Convex optimization based time-domain broadband beamforming with sidelobe control," *J. Acoust. Soc. Am.*, vol. 121, no. 1, pp. 46–49, Jan. 2007.

[6] J. Li and P. S. Eds., *Robust Adaptive Beamforming*. Hoboken, NJ, USA: Wiley, 2005.

[7] Y. Huang, W. Yang, and S. A. Vorobyov, "Robust adaptive beamforming maximizing the worst-case SINR over distributional uncertainty sets for random INC matrix and signal steering vector," in *Proc. ICASSP 2022 - 2022 IEEE Int. Conf. Acoust., Speech, Signal Process. (ICASSP), Singapore*, May. 2022, pp. 4918–4922.

[8] G. Huang, J. Benesty, J. Chen, and I. Cohen, "Robust and steerable kronecker product differential beamforming with rectangular microphone arrays," in *Proc. ICASSP 2020 - 2020 IEEE Int. Conf. Acoust., Speech, Signal Process. (ICASSP), Barcelona, Spain*, May. 2020, pp. 211–215.

[9] G. Huang, J. Chen, and J. Benesty, "Design of planar differential microphone arrays with fractional orders," *IEEE/ACM Trans. Audio, Speech, Lang. Process.*, vol. 28, pp. 116–130, Oct. 2019.

[10] W. Huang and J. Feng, "Differential beamforming for uniform circular array with directional microphones," in *Proc. INTERSPEECH 2020 - 21st Annual Conference of the International Speech Communication Association, Shanghai, China*, Oct. 2020, pp. 71–75.

[11] S. Yan, "Robust time-domain broadband modal beamforming for circular arrays," *IEEE Trans. Aerosp. Electron. Syst.*, vol. 56, no. 3, pp. 1783–1794, Jun. 2020.

[12] S. Yan, H. Sun, X. Ma, U. P. Svensson, and C. Hou, "Time-domain implementation of broadband beamformer in spherical harmonics domain," *IEEE Trans. Audio, Speech, Lang. Process.*, vol. 19, no. 5, pp. 1221–1230, Jul. 2011.

[13] H. Lebret and S. Boyd, "Antenna array pattern synthesis via convex optimization," *IEEE Trans. Signal Process.*, vol. 45, no. 3, pp. 526–532, Mar. 1997.

[14] S. Yan, Y. Ma, and C. Hou, "Optimal array pattern synthesis for broadband arrays," *J. Acoust. Soc. Am.*, vol. 122, no. 5, pp. 2686–2696, Nov. 2007.

[15] S. Yan, *Optimal Design of Time-Domain Broadband Beamformers*. Singapore: Springer Singapore, 2019.

[16] H. Chen, W. Ser, and Z. L. Yu, "Optimal design of nearfield wideband beamformers robust against errors in microphone array characteristics," *IEEE Trans. Circuits Syst. I, Reg. Papers*, vol. 54, no. 9, pp. 1950–1959, Oct. 2007.

[17] W. Wang, S. Yan, and L. Mao, "Time-domain frequency-invariant beampattern synthesis via alternating direction method of multipliers," *J. Acoust. Soc. Am.*, vol. 147, no. 5, pp. 3372–3375, May. 2020.

[18] W. Fan, J. Liang, G. Lu, X. Fan, and H. C. So, "Spectrally-agile waveform design for wideband MIMO radar transmit beampattern synthesis via majorization-ADMM," *IEEE Trans. Signal Process.*, vol. 69, pp. 1563–1578, Jan. 2021.

[19] J. F. Sturm, "Using SeDuMi 1.02, a Matlab toolbox for optimization over symmetric cones," *Optimization Methods and Software*, vol. 11, no. 1-4, pp. 625–653, Nov. 1999.

[20] M. Grant and S. Boyd, "CVX: Matlab software for disciplined convex programming, version 2.1," Mar. 2014, accessed on: May 20, 2023. [Online]. Available: http://cvxr.com/cvx.

[21] C. Olen and R. Compton, "A numerical pattern synthesis algorithm for arrays," *IEEE Trans. Antennas Propagat.*, vol. 38, no. 10, pp. 1666–1676, Oct. 1990.

[22] P. Y. Zhou and M. Ingram, "Pattern synthesis for arbitrary arrays using an adaptive array method," *IEEE Trans. Antennas Propagat.*, vol. 47, no. 5, pp. 862–869, May. 1999.

[23] X. Zhang, Z. He, B. Liao, X. Zhang, Z. Cheng, and Y. Lu, "$\mathrm{A^2RC}$: An accurate array response control algorithm for pattern synthesis," *IEEE Trans. Signal Process.*, vol. 65, no. 7, pp. 1810–1824, Apr. 2017.

[24] X. Zhang, Z. He, X.-G. Xia, B. Liao, X. Zhang, and Y. Yang, "OPARC: Optimal and precise array response control algorithm—Part I: Fundamentals," *IEEE Trans. Signal Process.*, vol. 67, no. 3, pp. 652–667, Feb. 2019.

[25] X. Ai and L. Gan, "Single-point array response control with minimum pattern deviation," in *Proc. ICASSP 2021 - 2021 IEEE Int. Conf. Acoust., Speech, Signal Process. (ICASSP), Toronto, Ontario, Canada*, Jun. 2021, pp. 4505–4509.

[26] R. Hunger, "Floating point operations in matrix-vector calculus," Technische Univ. München, München, Germany, Tech. Rep., 2007.

[27] J. B. Allen and D. A. Berkley, "Image method for efficiently simulating small-room acoustics," *J. Acoust. Soc. Am.*, vol. 65, no. 4, pp. 943–950, Apr. 1979.

[28] V. Zue, S. Seneff, and J. Glass, "Speech database development at MIT: Timit and beyond," *Speech Commun.*, vol. 9, no. 4, pp. 351–356, Jun. 1990.

[29] A. Varga and H. J. Steeneken, "Assessment for automatic speech recognition: II. NOISEX-92: A database and an experiment to study the effect of additive noise on speech recognition systems," *Speech Commun.*, vol. 12, no. 3, pp. 247–251, Jun. 1993.

[30] A. Rix, J. Beerends, M. Hollier, and A. Hekstra, "Perceptual evaluation of speech quality (PESQ) - a new method for speech quality assessment of telephone networks and codecs," in *Proc. ICASSP 2001 - 2001 IEEE Int. Conf. Acoust., Speech, Signal Process. (ICASSP), Salt Lake City, Utah, USA*, vol. 2, May. 2001, pp. 749–752.

[31] C. H. Taal, R. C. Hendriks, R. Heusdens, and J. Jensen, "An algorithm for intelligibility prediction of time–frequency weighted noisy speech," *IEEE Trans. Audio, Speech, Lang. Process.*, vol. 19, no. 7, pp. 2125–2136, Sep. 2011.